Computing (2010) 90:197–217
DOI 10.1007/s00607-010-0114-z

Improvements in retinal vessel clustering techniques: towards the automatic computation of the arterio venous ratio

S. G. Vázquez · N. Barreira · M. G. Penedo · M. Ortega · A. Pose-Reino

Received: 5 April 2010 / Accepted: 28 July 2010 / Published online: 22 August 2010

Abstract Retinal blood vessel structure is an important indicator for diagnosis of several diseases such as diabetes, hypertension, arteriosclerosis, or stroke. These pathologies cause early alterations in the blood vessels that affect veins and arteries differently. In this sense, the arterio venous ratio is a measurement that evaluates these alterations and, consequently, the condition of the patient. Thus, a precise identification of both types of vessels is necessary in order to develop an automatic diagnosis system, to quantify the seriousness of disease, or to monitor the therapy. The classification of vessels into veins and arteries is difficult due to the inhomogeneity in the retinal image lightness and the similarity of both structures. In this paper, several image feature sets have been combined with three clustering strategies in order to find a suitable characterization methodology. The best strategy has managed to classify correctly the 86.34% of the vessels improving the results obtained with previous techniques.

Communicated by G. Liotta.

S. G. Vázquez (✉) · N. Barreira · M. G. Penedo · M. Ortega
Department of Computer Science, University of A Coruña, A Coruña, Spain
e-mail: sgonzalezv@udc.es

N. Barreira
e-mail: nbarreira@udc.es

M. G. Penedo
e-mail: mgpenedo@udc.es

M. Ortega
e-mail: mortega@udc.es

A. Pose-Reino
Service of Internal Medicine, Hospital de Conxo, Santiago de Compostela, Spain
e-mail: antoniopose@telefonica.net

Keywords Vessel clustering · Arterio venous ratio

Mathematics Subject Classification (2000) 62H30 · 62H35 · 68T10

1 Introduction

With the development of the image processing techniques, the eye fundus image has become a very good tool of diagnosis because it is the unique part of human body where the micro-circulation can be see directly and non-invasively. Thus, the identification of fundus features, such as the optic nerve [1,2], the fovea [3,4], or the vessel tree [5,6], is an important research area since it helps the diagnosis of several pathologies. However, even though many solutions were proposed for the segmentation of the vessel tree, the distinction between veins and arteries is an open task. There are no algorithms that tackle it accurately because secondary vessels present homogeneous color, texture, and shape. Moreover, these features vary intra- and inter-patients. On one hand, there is a high color variation throughout the image due to inhomogeneous light reflections at the acquisition process. On the other hand, some biological characteristics, such as skin pigmentation, produce different retinal color patterns [7].

Nevertheless, a correct and precise labeling of the retinal vascular structure is necessary in order to develop automatic tools for diagnosis. For example, early changes in the retinal blood vessels are associated with several diseases, such as diabetes, hypertension or arteriosclerosis, that affect differently veins and arteries [8,9]. Some studies [10] associate the wider retinal venular caliber with hyperglycemia, diabetes and metabolic syndrome whereas retinal arteriolar narrowing was considered an early sign of hypertensive retinopathy. In this sense, the arterio venous ratio (AVR), this is, the ratio between the artery and vein calibers, is a well-known measurement for studying the retinal changes [11].

Even though the characterization of retinal vessels has not been much researched, we can find some methods in the literature that deal with this problem. These techniques can be classified into two categories: tracking-based and color-based methods. The former are semiautomatic since the medical experts have to label a few vessels and the system spreads the classification along the tree by means of a vessel tracking algorithm and the characterization of bifurcations and crossovers [12–14]. Their main advantage is the ability to classify the vessel tree completely. However, the performance depends highly on the quality of the segmentation and most of them need user interaction to correct the misclassifications of the significant points. The latter are automatic and they are based on color features since arteries are lighter than veins in the retinal images [15–18].

One of the first automatic methods was a Bayesian pixel classifier proposed by Simó and de Ves in 1999 [15] that distinguishes between background, fovea, veins and arteries. This method provides a good segmentation of the main vessels but it does not classify the little branches.

Li et al. [16] used a piecewise Gaussian model to describe the intensity distribution of line segments parallel to the vessel diameter. They use two Gaussian functions to

represent the vessel darkness and the vessel central reflex. They apply a supervised minimum distance classifier to these two dimensions to identify veins and arteries. The basis of their methodology is that the central reflex is more apparent in arteries than veins. However, the central reflex can only be observed in high-resolution images so their method cannot be applied to images with a low-resolution. In fact, they use a resolution of $3{,}072 \times 2{,}048$ pixels.

Grisan and Ruggeri [17] proposed a normalization of the retinal image and the division of the image into different regions to resolve the lightness and contrast problems. They identify the position of the optic disc and the cardinal axes that divide the retina into four quadrants. After that, they classify the vessels found in each quadrant separately. The mean of hue values in the HSL color space and the variance of red values in the RGB space are used as features to classify vessels via a fuzzy clustering algorithm. This algorithm is applicable as long as there are at least one artery and one vein in each quadrant. For this reason, they select five vessels in each quadrant. They obtained good results but 19.16% of the vessels were misclassified or unclassified since it is difficult to identify five vessels in each quadrant.

H.F. Jelinek et al. [18] tested different algorithms to characterize the retinal vessels in the vicinity of the optic disc. First, they detect the optic disc using a combination of Butterworth filtering, canny edge detection and morphological filters. The segmentation of the blood vessels is performed by tracking using a 2D non-linear least squares fitting. For the classification, they choose from ten to twelve vein and artery segments from three images. These segments represent the training set of 13 different classifier algorithms implemented in the Weka toolbox [19]. The best results were achieved with the Naïve–Bayes, the Decision Table and the J48 classifiers, obtaining an error of 30% at the test phases, which is significantly high.

Niemeijer et al. [20] proposed to discriminate the center-line pixels inside an artery from those inside a vein with a supervised method over a set of 12 features. They have used 20 images to train the algorithm, taking into account only the vessels which can be classified by experts through their color. An independent test of 20 images was used for testing. In this latter set, they obtained an area of 0.88 under a ROC curve. However this result is achieved without labeling small vessels.

In this work, we propose a simple methodology to characterize the retinal vessels in order to develop an automatic procedure for the computation of the arterio venous ratio. The lack of homogeneity and the uneven lightness are the main problems related to the retinal images and make the classification difficult. We have developed three different labeling strategies based on a clustering algorithm and we have tested several feature vectors. The first strategy classifies all vessels detected in the retinography. The second and the third strategies are based on the method proposed by Grisan and Ruggeri [17] since they classify subsets of detected vessels in order to reduce the effect of uneven lightness. On one hand, the second strategy divides the image into disjoint areas and classifies independently the vessels found in each area. On the other hand, the third strategy divides the image into several overlapped areas and combines the results obtained in the overlapped areas.

This paper is organized as follows. Section 2 presents the methodology for the vessel segmentation and the AVR computation. Section 3 explains the formal description of our technique. In Sect. 4, the experiments performed and the results obtained with

the three strategies are shown. Finally, Sect. 5 presents the conclusions and an outlook on future research directions.

2 Methodology for the AVR computation

The arterio venous ratio (AVR) is a measurement to quantify the variations in the caliber of the retinal vessels. It is widely used and several approaches have been proposed to calculate it. All of these methods share the measurement area, a concentric zone around the optic disc. However, they differ in the way the measurement is performed. The AVR has been computed as a ratio between the average arteriolar diameter and the average venous diameter [21] or by means of two measures, the central retinal artery equivalent (CRAE) and the central retinal vein equivalent (CRVE) [11,22–24]. Here we follow the first approach.

A semi-automatic methodology was proposed in [25] that consists of several stages. First, the optic disc is located within the retinal image and the analysis areas are defined. Second, the vessels are detected and segmented within the analysis areas. Finally, the vessel calibers are computed from the segmented vessels and the AVR is calculated using the vessel labeling provided by the expert.

The first stage in this methodology is the optic disc location. Even though this stage was performed at hand, there are several techniques in the literature that locate the optic disc automatically [26,27]. After that, several analysis radii are defined centered at the optic disc. For each radius r, two circumferences of radii $r - a$ and $r + a$, centered at the optic disc, define the analysis area where the vessels are detected.

In the second stage, the vessel segments are detected by means of a crease extraction algorithm [28]. If we consider the retinal image as a landscape, blood vessels can be seen as ridges or valleys, this is, regions that form an extreme and tubular level on their neighborhood. Thus, the vessels are detected from the crease lines in the analysis areas. Then, the segmentation of each vessel is performed of a specialized snake using the creases as the seed for the deformation. Once the snake is adjusted to the vessel boundaries, the snake contour points forms a parallelogram that surrounds the vessel segment, as Fig. 1 shows.

In the last stage, the vessel calibers are computed from the parallelograms. The expert labels the vessels as vein or artery and the AVR is automatically computed. Nevertheless, the manual vessel labeling is a time-consuming task and requires experience. The development of an efficient classification procedure will allow the development of automatic tools for the AVR computation in real-time, which will help the diagnosis and the screening of several pathologies.

3 Vessel classification

We propose a methodology based on color for the automatic vessel classification in the AVR computation problem. This methodology combines two elements: a clustering algorithm and a procedure to perform the classification. Nevertheless, the classification is not straightforward since both types of vessels presents very similar distributions of pixel colors, as Fig. 2 shows. For this reason, we should identify robust features to

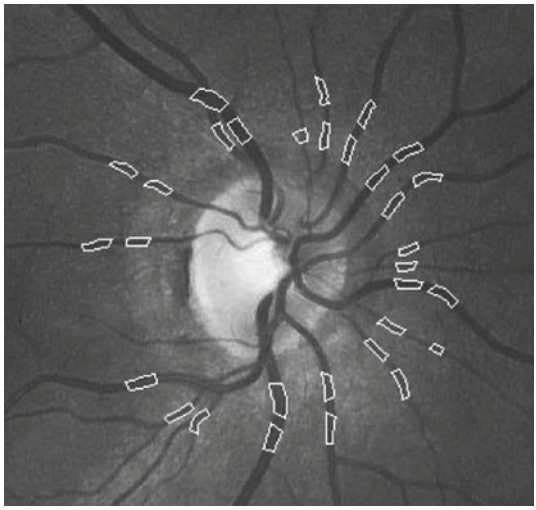

Fig. 1 Results of the segmentation process in two different radii. Each detected vessel is defined by a parallelogram

characterize both types of vessels. This section analyzes several image features and presents the proposed classification methodologies.

3.1 Feature vectors

The AVR is computed from vessel segments extracted at different interest radii. Hence, the classification will be focused on these vessel segments bounded by parallelograms. The labeling of the whole vessel tree is unnecessary for the AVR computation and requires a higher computational effort.

The first step in any classification process is to define the features for the classification. Our vessel classification procedure is based on the vessel color since the experts base their classifications on the fact that the arteries are lighter than the veins. We have analyzed different color spaces, in particular, RGB, HSL and gray level. The gray scale was computed as a linear combination of the three channels in RGB color model ($Gray = 0.2999 \times R + 0.587 \times G + 0.114 \times B$). The blue component (B) in the RGB model as well as the saturation (S) and lightness (L) components in the HSL model were discarded due to their little contrast as Fig. 3 shows.

Moreover, we can define three types of features from the vessel segments regarding the involved pixels:

- Features based on the whole vessel segment, e.g. the mean of the vessel segment pixels in a given color component.
- Features based on each profile pixel. We have considered the pixel value in a color component or the combination of pixel values in several color components for all pixels in each profile.
- Features based on groups of pixels. We have considered features based in each cross section of the vessel segments, the so-called *profiles* (Fig. 4). We can compute a measurement from the profile, such as the mean or the median, or we can

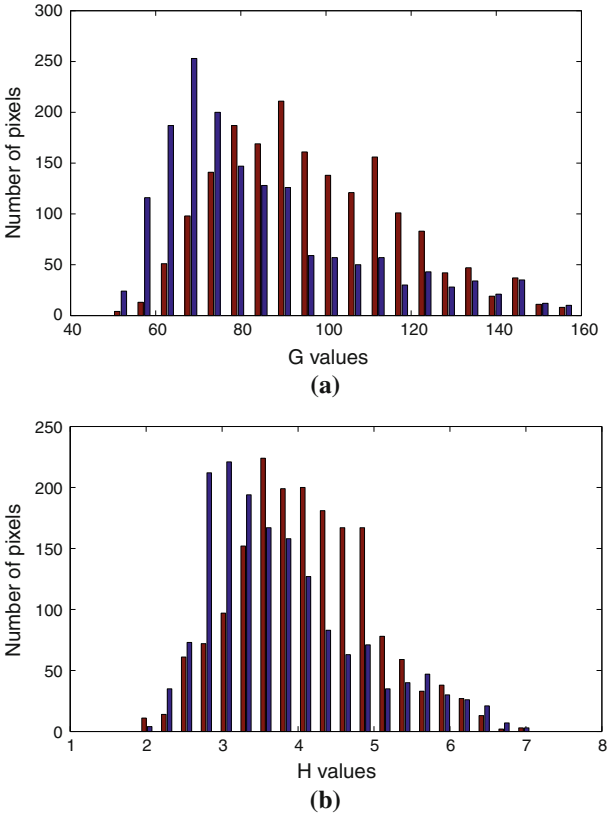

Fig. 2 Distribution of pixel colors in both artery and vein segments in a retinal image. The histograms were computed using **a** the green component and **b** the hue component from the RGB and HSL color spaces, respectively. The arteries (*red*) are, on the whole, lighter than the veins (*blue*). However, both color distributions are mixed (color figure online)

select several values to represent the profile, e.g., the n most repeated values in the profile pixels.

We have discarded the features based on the whole vessel segments due to the variation within a class. Moreover of the features mentioned above, we have analyzed another feature vector proposed by Grisan and Ruggeri [17] which consists of two components, the mean of the H component and the variance of the R component in the profile. This list summarizes the feature vectors that we have finally used:

- Pixel based features
  - One single value: (R), (G), (H), $(Gray)$
  - Combination of values: (G, R)
- Profile based features
  - One single value:
    - Mean: $(\mu(X))$ where $X \in \{R, G, H, Gray\}$
    - Median: $(\tilde{x}(X))$ where $X \in \{R, G, H, Gray\}$

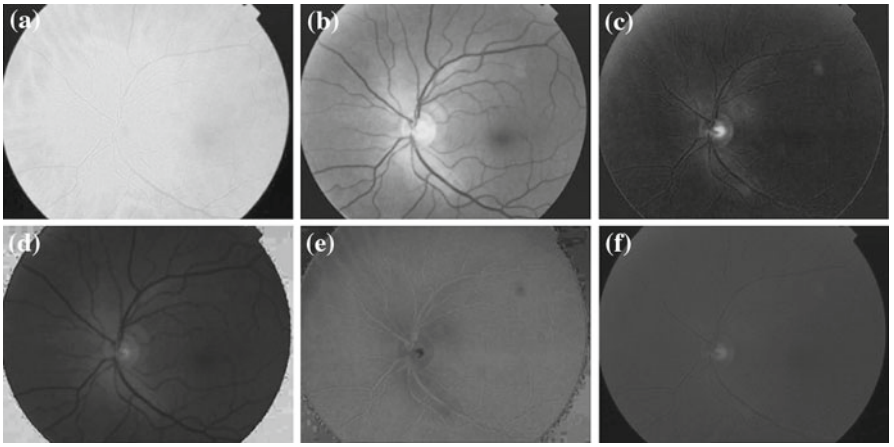

Fig. 3 Decomposition of a retinography in RGB and HSL color components, being **a**, **b** and **c**, R, G and B components from the RGB color space, respectively and **d**, **e** and **f**, the components H, S, and L from the HSL color space

Fig. 4 Several profiles extracted from a vessel segment

- n most repeated values: $(X_1), (X_2) \ldots (X_n)$ where $X \in \{R, G, H, Gray\}$
- Mean of n most repeated values: (μ(n most repeated values(X)) where $X \in \{R, G, H, Gray\}$

– Combination of values:
  - n most repeated values: $(G_1, R_1), (G_2, R_2) \ldots (G_n, R_n)$
  - Mean of n most repeated values: (μ(n most repeated values(G)), μ(n most repeated values(R)))
  - Mean of H and variance of R (Grisan et al.'s features): $(\mu(H), \sigma(R))$

3.2 Vessel labeling

The feature vectors previously computed are the input of a clustering algorithm that decides the type of vessel that they represent. After that, we decide the type of the vessel segment taking into account all the feature vectors related to this vessel segment.

We have applied an unsupervised clustering algorithm since the uneven intra-image contrast and lightness makes difficult the use of a supervised algorithm. We have selected the k-means algorithm [29] due to its simplicity, computational efficiency, and few parameter tuning. Since there are only two clusters whose centers should be as far as possible to obtain a good classification, we initialize the centroids of each class to the maximum and minimum values of the input set, respectively. We have developed three different strategies to obtain the centers of the clusters vein and artery:

1. We classify all vessels segments detected together, so we obtain two centers of cluster, one per each category.
2. We divide the image into four disjoint areas and classify the vessel segments in each area, so we get four centers of cluster for each category.
3. We divide the image into overlapping regions and we apply the classification algorithm in each region independently. In this case, the vessel segments can belong to several regions and can be classified several times.

3.2.1 Strategy 1

In the first approach, all the vessel segments that were detected in each circumference are classified together, this is, we apply k-means to the full feature vector set. After that, we obtain the centers of the vein and artery classes. We use the Euclidean distance to classify each feature vector as vein or artery. When all the feature vectors are classified, we calculate the empirical probability P of the vessel segment to be a vein or an artery as follows:

$$P[v_i \in \text{Artery}] = \frac{n_{a_i}}{n_{a_i} + n_{v_i}}, \quad P[v_i \in \text{Vein}] = \frac{n_{v_i}}{n_{a_i} + n_{v_i}} \tag{1}$$

where v_i is the i-th vessel segment, n_{a_i} the number of feature vectors from the vessel segment i that were classified as artery and n_{v_i} is the number of feature vectors that were classified as vein.

Finally, we add the vessel to the class with the highest probability. If the probability values of vein and artery are the same, we do not classify that vessel.

The main drawback of this approach is the lightness and contrast variability in the retinal images. The vessel color on the left area is very different from the vessel color on the right area, even though both vessels belong the same class. Figure 5 shows the result of classifying a retinal image with this strategy. Note how the left area is darker than the right area, so this algorithm labels all the vessels on the left as vein and the vessels on the right as artery. However, this strategy works correctly in the retinography of Fig. 6 because the lightness is more uniform. Figure 7 shows the manual labeling of these retinographies.

3.2.2 Strategy 2

To overcome the limitations of the previous strategy, we test a second strategy based on the method proposed by Grisan and Ruggeri [17]. We divide the retina fundus image in four quadrants centered at the optic disc and we apply the k-means to the

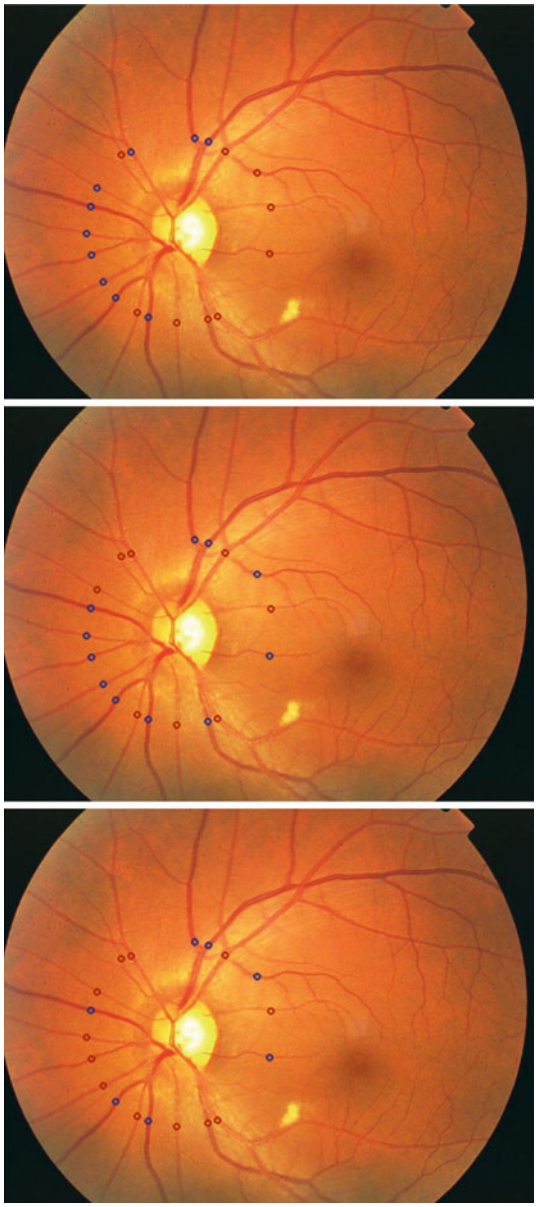

Fig. 5 From *top to bottom*, classification results in a sample image using strategies 1, 2, and 3. The *blue circles* represent veins whereas the *red circles* point out arteries. Note how the first strategy classifies all left vessels as veins and right vessels as arteries because the left area is darker than the right area. The second strategy improves the results but all vessels at the bottom left are classified as veins, too. The third strategy avoids the problem of the uneven lightness (color figure online)

feature vectors found in each quadrant independently. Since the k-means algorithm needs samples of each class to work correctly, this method is applicable as long as there are at least a vein and an artery in a quadrant. Thus, we demand, at least, three detected vessels in a quadrant. This solution minimizes the number of false positive and false negative but a high number of vessels cannot be classified.

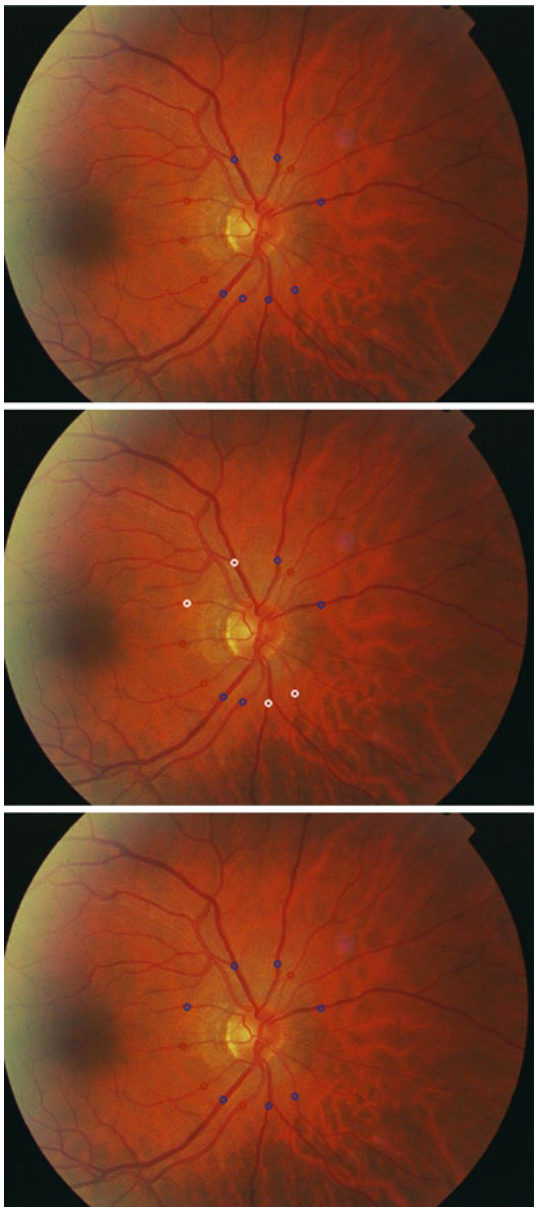

Fig. 6 From *top to bottom*, classification results in a sample image using strategies 1, 2, and 3. The *blue circles* represent veins, the *red circles* point out arteries, and the *white points* are unclassified vessels. The second strategy cannot classify vessels in the second and fourth quadrants because less than three vessels were found in these quadrants (color figure online)

After the classification of all the feature vectors in each quadrant, the vessel segment labeling is performed in the same manner as the previous strategy.

Figures 5 and 6 show sample images classified with this strategy. In the first image, the division of the image into quadrants is not enough to avoid the uneven lightness effect and causes several misclassifications. The second image shows how the lack of vessels does not allow the vessel classification in the second and fourth quadrants.

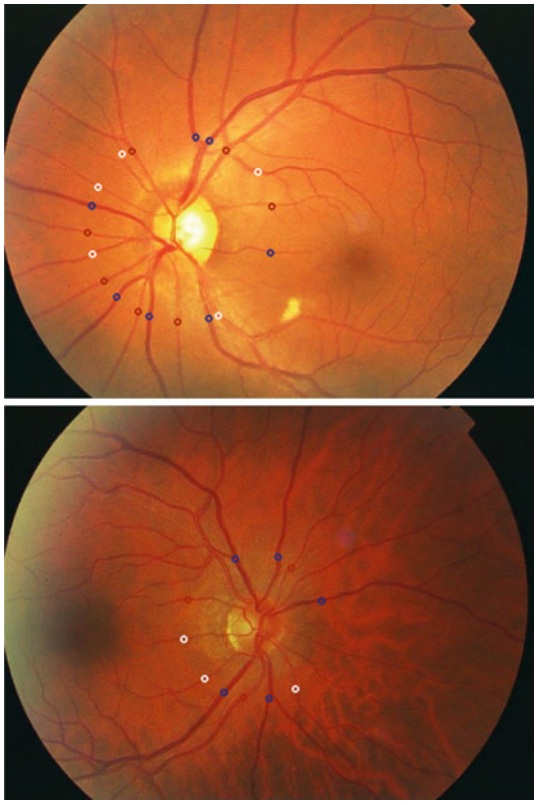

Fig. 7 Manual labeling of the retinographies shown in the Figs. 5 and 6. The *blue circles* represent veins, the *red circles* are arteries, whereas the *white circles* are the unclassified vessels (color figure online)

3.2.3 Strategy 3

In this strategy, the image is divided into overlapping regions to minimize the influence of uneven lightness and the number of unclassified vessel segments. First, we divide the retina fundus image in four quadrants and then we rotate the coordinate axis through an angle of 20° between 0° and 180°. This way, we obtain different quadrants as can be seen in the Fig. 8. Next, we apply the k-means clustering algorithm to the feature vectors that belong to the vessel segments found in each quadrant. In consequence, a feature vector can be classified several times in different quadrants.

For each vessel segment, the final vein and artery probabilities are computed as the mean of the probabilities in all the quadrants where the vessel segment was found and classified. Then, we select the class with the highest probability as the vessel segment type. As before, if both vein and artery probabilities are equal, we do not classify the vessel.

Figures 5 and 6 show two retinographies labeled with this strategy. We can see that this strategy obtains the best vessel characterization.

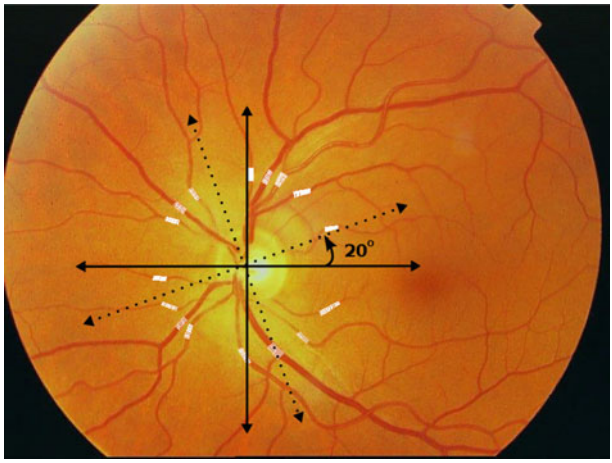

Fig. 8 Division of the retinal images by rotation of the coordinate axes

4 Results

In this section we show the classification results achieved with the different strategies and the proposed feature vectors. We have tested the proposed methodology on two different data sets. The first set is made up of 20 retinal images whereas the second one has 58. The images of both sets were captured without pupil dilation at the Service of Internal Medicine of Hospital de Conxo in Santiago de Compostela from a Cannon CR6-45NM non-mydriatic retinal camera. All the images are centered in the optic disc and have a resolution of 768 × 576 pixels. To assess the validity of the method, we have considered the following measures:

- *Sensitivity* and *specificity* of the system to detect the veins and arteries (Sens_v, Sens_a, Spec_v, Spec_a). The sensitivity measures the proportion of actual positives which are correctly identified and the specificity measures the proportion of negatives which are correctly identified. A vessel segment is considered as a positive vein (artery) if its probability to be vein (artery) is greater than 0.5.
- The *accuracy rate*, the percentage of the vessel segments which have been correctly classified penalizing with the vessels unclassified by the system.

$$\text{Accuracy rate} = \frac{n_{\text{corrected-classifications}}}{n_{\text{vessels}}} * 100 \tag{2}$$

where $n_{\text{corrected-classifications}}$ is the number of vessel segments, veins and arteries, correctly classified and n_{vessels} is the total number of detected vessel segments that includes the number of vessel segments which have not been able to classify.

4.1 Tuning results

In the tuning phase, we have used a set of 20 images from VICAVR database [30] where the blood vessels have been manually classified by a medical expert using a

web application that computes the AVR [31]. The classification results achieved by the proposed strategies on the data set were compared to the manual classification results.

According to previous studies of AVR ratio [11,21,24,32] and the experts' argument, the classification task was performed in three different analysis radii of 2, 2.5 and 3 times the optic disc radius. The experts consider the vessel diameter becomes too small in higher radii and makes difficult a correct classification. Even the medical experts need to perform a vessel tracking from the optic disc in order to classify correctly the small vessels. In this data set, the expert has not labeled all the vessel segments which the system had detected. Only certain vessels (up to a number that allows the AVR computation) that could be identified as vein or artery have been classified. In our image set, a total of 193, 203 and 206 vessel segments were labeled at each radius.

We denote by r the optic disc radius to simplify the nomenclature.

4.1.1 Analysis of strategies

In this section, we analyze the performance of the system with respect to the proposed strategies and feature vectors in the three analysis radii in order to determine which is the method that obtains the best classification.

We use the color information of all the points in each profile as feature vectors in order that the k-means algorithm would have more information to classify. Also, we use a feature based on a group of vessel pixels, the mean of H component and the variance of R component of the profiles [17].

Figure 9 shows the accuracy rate obtained with each strategy in the tuning phase. In the three strategies, the best results were achieved with the H, G and the union of G and R components, whereas the worst results were obtained with the R component and the union of the mean of H and variance of R. In addition, the accuracy rate decreases with the radius because the images get blurred and the vessel diameters become small, but we can obtain good results up to 2.5 times the radius. It is worth to point out that the low accuracy rate in the second strategy is due to the high number of unclassified vessels mainly. The optimal strategy is the third one because the classification error is the lowest and a high number of vessels is classified. This latter point is due to the fact that the algorithm classifies all detected vessels except for some rare cases, such as when the vein and artery probability values coincide or when there are less than three vessels in all quadrants where the vessel is found.

4.1.2 Analysis of statistical measures on the color components in a radius 2.5r with the strategy 3

In the previous experiment, the results have proved that the strategy 3 is the best one and a suitable analysis radius is 2.5 times the optic disc because the misclassifications and the number of unclassified vessels were the lowest ones. Thus, in this experiment, we try to minimize the error committed with this strategy in that radius. To this end, instead of considering the component values in all the points of the profiles, we analyze different statistical measures on the components to minimize the effect of both noise and outliers in the profile lightness information. So, we study the average, the median of all the values in the profile, the five most repeated values in the profile and

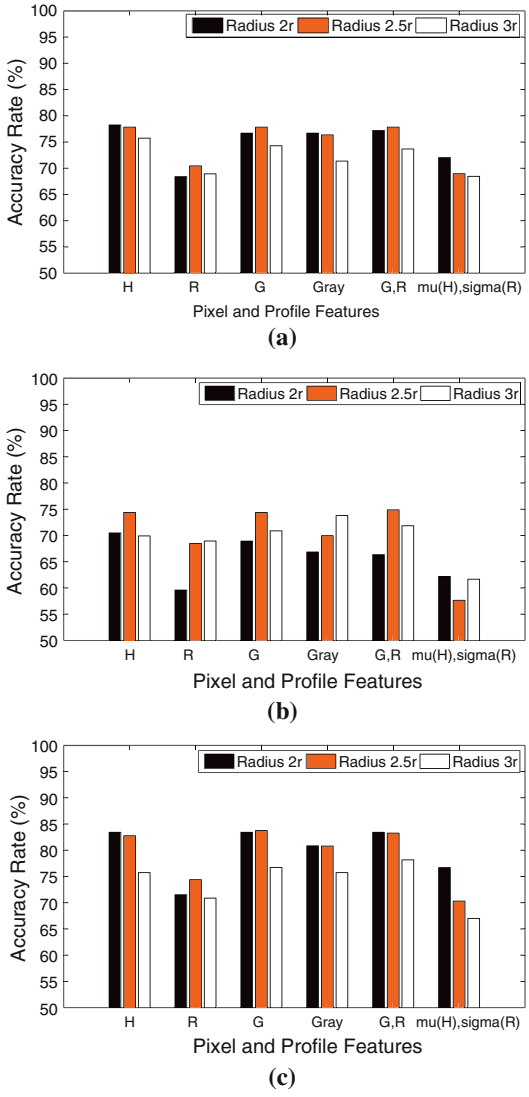

Fig. 9 Vessel classification performance using **a** strategy 1, **b** strategy 2 and **c** strategy 3, in different analysis radii and distinct feature vectors on the data set of 20 images

the mean of the five most repeated values. The classification performance using these feature vectors can be seen in Fig. 10. The G component of the RBG color model is the most discriminant color component with all statistical measures. The best classification results were achieved using the mean of the G component since the error rate was reduced to 12.38%.

4.1.3 Analysis of the G component in several radii with different feature vectors

Taking into account the results obtained in the previous analysis, the component G of the RGB model provides the best classification using the best strategy. This is due to

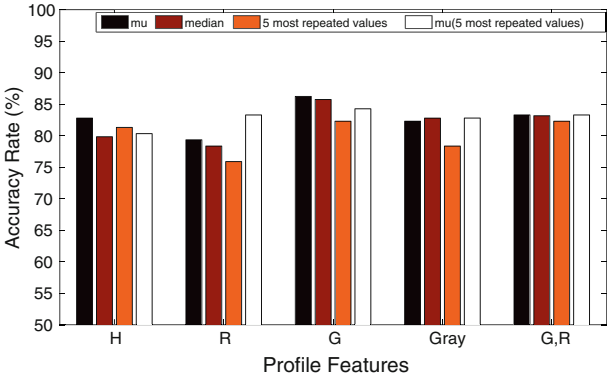

Fig. 10 Vessel classification performance with the strategy 3 in a radius 2.5r using different feature vectors on the data set of 20 images

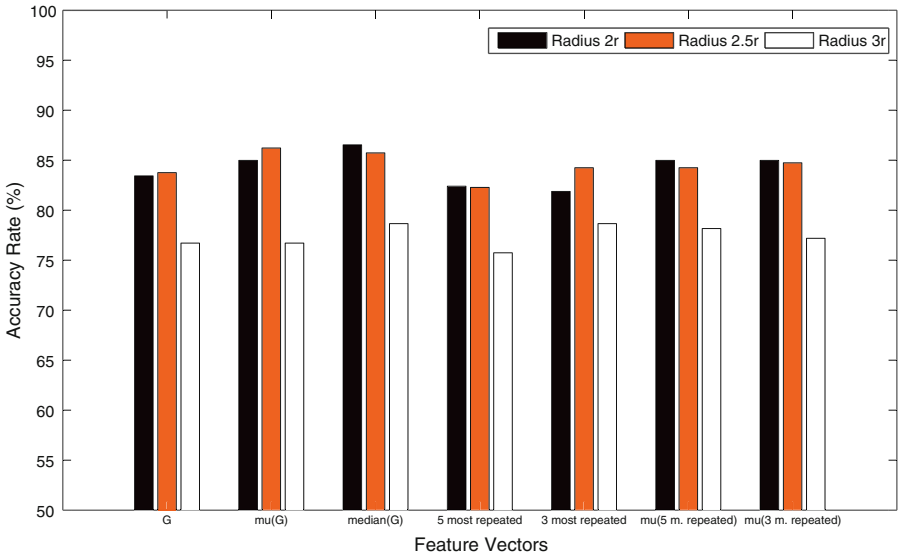

Fig. 11 Vessel classification performance with the strategy 3 in three analysis radii using distinct profile features based on the G component on the data set of 20 images

the contrast of the G channel is higher than the others components and makes possible to increase the distance between the artery and vein clusters.

Figure 11 shows the classification performance with the strategy 3 in three analysis radii using several profile features on the G component. The best labeling accuracy is obtained using the median of the G component in a radius 2r. For 2.5r, the error achieved with the mean is lower but, for the other radii, the median results are better. However, since the results obtained are so similar, we can consider both features are good to discriminate between veins and arteries.

Table 1 The percentage of the agreement between the three experts (E1, E2, E3) in the VICAVR data set

	E1	E2	E3
E1	–	98.12%	96.69%
E2	–	–	97.37%
E3	–	–	–
Three-agreement	96.53%		

4.2 Test results

The best accuracy rates at the tuning phase were 86.53 and 86.21% in the radii 2r and 2.5r using the median and the mean of the G component, respectively. To confirm these results, we have tested the third strategy with the mean and the median of the G component in a public data set called VICAVR [30]. This data set contains 58 retinal images centered on the optic disc. Each image was labeled by three different medical experts separately using the web application described in [31]. However, in this case, the experts have labeled all detected vessel segments except those which could not be identified as vein or artery.

In the tuning phase, we have concluded that the radius 2.5r was suitable to classify the vessels because in higher radii the number of misclassifications increased. In this way, in the test phase, we have considered this radius as the last one, instead of the radius of 3r because the higher radius do not contribute in the AVR calculus and the results are worse. Moreover, in order to test our classification approach with a high number of samples, we have divided the region of interest in five circumferences instead of three. Thus, in this data set, the experts have labeled the same vessel segments detected in the five circumferences concentric to the optic disc. The radii of the circumferences are equally spaced and they range from 1.5r to 2.5r, where r is the optic disc radius. From 3,816 vessel segments, the experts were able to label 2,471, 2,778, and 2,943 vessels, respectively. The agreement between experts is considerably high as Table 1 shows.

Considering the agreement between the three experts as the gold standard, the accuracy rate obtained was 86.34% using the median of the G component in the profile and 85.68% with the mean. Figure 12 shows the ROC curve of the classifier respect to this gold standard. The curve has been computed taking into account different thresholds of the probability to consider a result as positive. An area under the curve of 0.93 indicates that the system's accuracy is good. In addition, this graph shows that the best thresholds to balance sensitivity and specificity in the test set are 0.7. However, depending on the application domain, it may be interesting to increase both threshold values (vein and artery probabilities) and to introduce an unclassified interval, i.e., decreasing the sensitivity and increasing the specificity, in order to minimize the error. Table 2 shows the sensitivity and specificity of veins and arteries if both threshold values are 0.7. In this case, the percentage of the unclassified vessels increases to 14.13% whereas the misclassification rate falls to 8.81%.

Table 3 summarizes the results obtained with our methodology at the tuning and the test phases and the results achieved by other techniques found in the literature. Grisan and Ruggeri's method gets a low percentage of misclassifications (12.4% error)

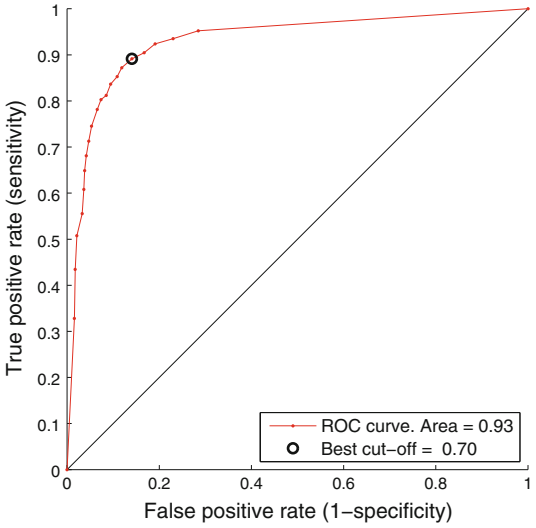

Fig. 12 ROC curve in the VICAVR data set computed using different threshold probability values and considering the agreement between the three experts as the gold standard

Table 2 Sensitivity and specificity of veins and arteries in the VICAVR data set using the third strategy and the median of the G component in the profiles. The thresholds of artery and vein probabilities were 0.7

Expert	Vessel labeled	Sens_v	Spec_v	Sens_a	Spec_a
Three-agreement	2,116	88.15%	87.21%	67.01%	96.99%

Table 3 Vessel classification performance comparative among the techniques found in the literature

Technique	Clustering algorithm	Accuracy rate
Grisan and Ruggeri [17]	Fuzzy clustering	79.88%
H.F. Jelinek et al. [18]	Naïve–Bayes	69%
	Decision Table	70%
	J48	70%
Niemeijer et al. [20]	K-Nearest Neighbor	0.88 (ROC curve area)
Our method	K-means	86.53% (set of 20 images)
		86.34% (set of 58 images)

without much computational cost, however the strict division in quadrants forces to unclassify a high number of vessels (7.70%) and makes the labeling of a vessel very dependent on the vessel neighbors. The error rates obtained by H. F. Jelinek et al. are high. Finally, the results of Niemeijer et al. are not comparable because they only take into account the main vessels and the problems arise with thinner vessels.

To make a more precise comparison with the methods above mentioned, we have tested these approaches in the VICAVR data set using as the gold standard the

agreement among the three experts. First, the method proposed by Grisan et al. is similar to the second strategy analyzed in this work using the feature vector made up of the mean of the H component and the variance of the R component in the profile. The accuracy rate obtained in the VICAVR data set was 53.63% using the strategy and the feature set previously mentioned. The percentage of vessels correctly classified was 64.21%, thus, there were almost a 10% of unclassified vessels.

We have also applied the methodology proposed by Jelinek et al. in the VICAVR data set. First, we applied a gross median filter to estimate the background of each channel and then we subtracted this estimation from the channel. However, since we do not know the camera aperture used in the capture process of the VICAVR images, we could not apply their algorithm to adjust the image histograms. Thus, we use the normalized images to compute the proposed features (mean and standard deviation of H, G, R and B) from our profiles and apply the Correlation-based Feature Subset Evaluation method of Weka. The features selected by this method in the VICAVR data set were the mean and standard deviation of G, the standard deviation of R, and the standard deviation of H. We have tested these features, as well as the features selected in their data set with the proposed classifiers (Naïve Bayes, DecisionTable and J48) implemented in Weka toolbox using a 10-fold cross-validation. The percentage of correctly classified instances for our features was 65.15% with Naïve Bayes, 73.80% with the Decision Table and 77.79% using J48. The results using the features chosen by the Correlation-based Feature Subset Evaluation method in their data set (the mean of G and the mean and the standard deviation of H) were 64.82, 67.63, and 68.15%, respectively. These results are similar to those achieved by Jelinek et al. in both cases.

Finally, according to Niemeijer et al., we have tested the artery and vein classification with Support Vector Machines (SVM's) using a 5–5 fold cross-validation. To this end, we have analyzed a big set of features similar to those used by Niemeijer et al. except for the steerable filters. These features consist of color features (the mean and the median of profile values in each component of the RBG and HSL color spaces, the central value of the profile, the mean and the median of crease values,…), contrast features (the standard deviation of the profile and crease values), shape features (skewness and kurtosis of the profiles) and quality features (the caliber of the vessel, the features previously mentioned normalized by their value in the image or normalized by the caliber of the vessel). We have applied several feature selection methods of the Weka toolbox before classifying the feature vectors with SVM. The best percentage of correctly classified instances was 78.54% and it was achieved with 12 features selected by the correlation-based Feature Subset Evaluation method. The selected features were the standard deviation of H in the profile, the median of G and H components in the profile normalized by the caliber, the median of G in the profile normalized by their value in each image, the standard deviation of G in the crease, the mean of H in the crease, the G value in each point of the crease, the caliber, the caliber normalized by their value in the image, the 10th percentile of the H component in the profile and the skewness of G in the profile.

As a conclusion, the best percentages of correctly classified vessels in the VICAVR data set were obtained with our approach.

4.3 Computation times

The algorithms have been implemented in C++ and the analysis have been performed in a PC running Debian GNU/Linux, with an 2.4 GHz Intel Pentium 4 processor and 512 Mb of RAM.

The computation time for an image depends on the times that the k-means clustering algorithm is executed, i.e., depends on which strategy is used. For a 768×576 image, the computation time is one second with the first and second strategies and 2 seconds with the third one.

5 Conclusions

We have developed a new methodology to classify the retinal vessels into arteries and veins. To this end, we have analyzed three different clustering strategies and we have tried out several feature vectors based on the color information of the pixels in the fundus image. The first strategy classifies globally all detected vessels applying a clustering algorithm once. The second one divides the retinal image into four quadrants and classifies the vessels that belong to the same quadrant independently of the rest of vessels. The third strategy classifies the vessels dividing the retinal image into quadrants that are rotated.

Several feature vectors based on the RGB, HSL, and gray scale models have been analyzed in order to obtain a precise vessel characterization.

The results have proved that the best strategy is the third one because it minimizes the error rate and the number of unclassified vessels whereas the most discriminant feature vector is based on the mean or the median of the green component of the RGB color space.

For a data set of 20 images, we have classified correctly the 86.53% of the vessels and this percentage of correctly classified vessels remains almost constant in a test set of 58 images labeled by three medical experts. Thus, we have improved the percentage of vessels classified correctly regarding other techniques in the bibliography and, at the same time, the number of unclassified vessels was reduced. Moreover, these results were achieved applying a fast and simple algorithm without a preprocessing step.

Several future research directions could be of interest. The purpose of this work is the development of a system that computes the arteriolar-to-venular (AVR) diameter ratio automatically. To this end, we need to combine our methodology with an algorithm for the automatic location of optic disc. Moreover, the classification error rates can be reduced considering possible improvements. On one hand, this method can be combined with tracking algorithms to classify the vessels in different analysis radii to ensure the category of the vessel. On the other hand, the development of a good normalization algorithm can improve the gap between the lightness in arteries and veins and, this way, can increase the accuracy of the results.

Acknowledgments This work has been partly funded by the Fondo de Investigación Sanitaria (Ministerio de Ciencia e Innovación, Spain) through the grant contract ETES-FIS 08/90420 with FEDER funds.

References

1. Hoover A, Goldbaum M (2003) Locating the optic nerve in a retinal image using the fuzzy convergence of the blood vessels. IEEE Trans Biomed Eng 22:951–958
2. Blanco M, Penedo MG, Barreira N, Penas M, Carreira MJ (2006) Localization and extraction of the optic disc using the fuzzy circular Hough transform. Lect Notes Artif Intell Artif Intell Soft Comput 4029:713–721
3. Li H, Chutatape O (2004) Automated feature extraction in color retinal images by a model based approach. IEEE Trans Biomed Eng 51:246–254
4. Penedo MG, Pena S, González F (2008) Crest lines and correlation filter based location of the macula in digital retinal images. BIOSIGNALS 2:521–527
5. Soares JVB, Leandro JJG, Cesar RMJr, Jelinek HF, Cree MJ (2006) Retinal vessel segmentation using the 2-D Gabor wavelet and supervised classification. IEEE Trans Med Imaging 25(9):1214–1222
6. Salem SA, Salem NM, Nandi AK (2007) Segmentation of retinal blood vessels using a novel clustering algorithm (RACAL) with a partial supervision strategy. Med Biol Eng Comput 45(3):261–273
7. Cree MJ, Gamble E, Cornforth D (2005) Colour normalisation to reduce inter-patient and intra-patient variability in microaneurysm detection in colour retinal images. WDIC2005 ARPS workshop on digital image computing, Brisbane, Australia, pp 163–168
8. Stanton AV, Wasan B, Cerutti A, Ford S, Marsh R, Sever PP, Thom SA, Hughes AD (1995) Vascular network changes in the retina with age and hypertension. J Hypertens 13:1724–1728
9. King LA, Stanton AV, Sever PS, Thom SA, Hughes AD (1996) Arteriolar length–diameter (l:d) ratio: a geometric parameter of the retinal vasculature diagnostic of hypertension. J Hum Hypertens 10(6): 417–418
10. Nguyen TT, Wang JJ, Wong TY (2007) Retinal vascular changes in pre-diabetes and prehypertension: new findings and their research and clinical implications. Diabetes Care 30(10):2708–2715
11. Hubbard LD, Brothers RJ, King WN, Clegg LX, Klein R, Cooper LS, Sharrett AR, Davis MD, Cai J (1999) Methods for evaluation of retinal microvascular abnormalities associated with hypertension/sclerosis in the atherosclerosis risk in communities studies. Ophthalmology 106:2269–2280
12. Aguilar W, Elena Martínez-Pérez M, Frauel Y, Escolano F, Lozano MA, Espinosa-Romero A (2007) Graph-based methods for retinal mosaicing and vascular characterization. In: GbRPR. Lecture Notes in Computer Science, vol 4538. Springer, Berlin, pp 25–36
13. Chráastek R, Wolf M, Donath K, Niemann H, Michelsont G (2002) Automated calculation of retinal arteriovenous ratio for detection and monitoring of cerebrovascular disease based on assessment of morphological changes of retinal vascular system. IAPR Workshop on Machine Vision Applications, Nara, Japan 11–13, pp 240–243
14. Rothaus K, Jiang X, Rhiem P (2009) Separation of the retinal vascular graph in arteries and veins based upon structural knowledge. Image Vis Comput 27(7):864–875
15. Simó A, Ves Ede (2001) Segmentation of macular fluorescein angiographies. A statistical approach. Pattern Recognit 34(4):795–809
16. Li H, Hsu W, Lee ML, Wang H (2003) A piecewise Gaussian model for profiling and differentiating retinal vessels. In: ICIP03, vol 1, pp 1069–1072
17. Grisan E, Ruggeri A (2003) A divide et impera strategy for automatic classification of retinal vessels into arteries and veins. In: Engineering in Medicine and Biology Society, 2003. Proceedings of the 25th Annual International Conference of the IEEE, vol 1, pp 890–893
18. Jelinek HF, Lucas C, Cornforth DJ, Huang W, Cree MJ (2005) Towards vessel characterization in the vicinity of the optic disc in digital retinal images. In: McCane (ed) Proceedings of the image and vision computing, New Zealand
19. Hall M, Frank E, Holmes G, Pfahringer B, Reutemann P, Witten IH (2009) The WEKA data mining software: an update. SIGKDD Explor 11(1):10–18. http://doi.acm.org/10.1145/1656274.1656278. DBLP, http://dblp.uni-trier.de
20. Niemeijer M, van Ginneken B, Abràmoff MD (2009) Automatic classification of retinal vessels into arteries and veins. In: Karssemeijer N, Giger ML (eds) Medical imaging 2009: computer-aided diagnosis. Proceedings of the SPIE, 7260:72601F–72601F–8
21. Stanton A, Mullaney P, Fainsia M, O'Brien E, O'Malley K (1995) A method of quantifying retinal microvascular alterations associated with blood pressure and age. J Hypertens 13(1):41–48
22. Parr JC, Spears GF (1974) General caliber of the retinal arteries expressed as the equivalent width of the central retinal artery. Am J Ophthalmol 77:472–477

23. Parr JC, Spears GF (1974) Mathematic relationships between the width of a retinal artery and the widths of its branches. Am J Ophthalmol 77:478–483
24. Knudtson MD, Lee KE, Hubbard LD, Wong TY, Klei R, Klein BEK (2003) Revised formulas for summarizing retinal vessel diameters. Curr Eye Res 27(3):143–149
25. Caderno IG, Penedo MG, Barreira N, Mariño C, González F (2005) Precise detection and measurement of the retina vascular tree. Pattern Recognit Image Anal Adv Math Theory Appl (IAPC Nauka/Interperiodica) 15(2):523–526
26. Blanco M, Penedo MG, Barreira N, Penas M, Carreira MJ (2006) Localization and extraction of the optic disc using the fuzzy circular hough transform. In: Rutkowski L, Tadeusiewicz R, Zadeh LA, Zurada JM (eds) ICAISC. Lecture Notes in Computer Science, vol 4029. Springer, berlin, pp 712–721
27. Novo J, Penedo MG, Santos J (2009) Localisation of the optic disc by means of ga-optimised topological active nets. Image Vis Comput 27(10):1572–1584
28. López AM, Lloret D, Serrat J, Villanueva JJ (2000) Multilocal creaseness based on the level-set extrinsic curvature. Comput Vis Image Understand 77(2):111–144
29. Gan G, Ma C, Wu J (2007) Data clustering theory, algorithms and applications. ASA-SIAM Series on Statistics and Applied Probability, SIAM, Philadelphia, ASA, Alexandria, VA
30. VICAVR (2009) VARPA Images for the Computation of the Arterio/Venular Ratio, database. http://www.varpa.es/vicavr.html
31. Mariño C, Penedo MG, Rouco J, Ortega M, Pose-Reino A (2008) Medical web application for the evaluation of changes in retinal microcirculation. Comput Eng Syst Appl 113–119
32. Pose-Reino A, Gomez-Ulla F, Hayik B, Rodriguez-Fernndez M, Carreira-Nouche MJ, Mosquera-Gonzlez A, Gonzlez-Penedo M, Gude F (2005) Computerized measurement of retinal blood vessel calibre: description, validation and use to determine the influence of ageing and hypertension. J Hypertens 23(4):843–850